FORMULATION AND DEVELOPMENT OF NEBIVOLOL HYDROCHLORIDE LOADED CHITOSAN-PLGA BASED NANOGEL: EX VIVO PERMEATION AND IN VIVO PHARMACOKINETIC STUDY

Parameshwar Kondapuram [a, b], Dr. Suvendu Kumar Sahoo[a]*

Article History: **Received:** 23.09.2022 **Revised:** 23.10.2022 **Accepted:** 03.11.2022

Abstract: Nebivolol hydrochloride (NBH) chitosan-PLGA loaded nanoparticles obtained using the nanoprecipitation/solvent displacement process in the present study, characterization by P-XRD, DSC, SEM, and FTIR analytical techniques. During *the in-vitro* drug release, *ex-vivo* permeation studies. The nanoparticles prepared to employ 150mg chitosan, 100mg PLGA, and 1:5 H_2O: CH_2Cl_2 incorporated with NBH showed a high drug entrapment of approximately 94%, with an average particle diameter of 180.32 nm and zeta potential of −30.40±0.12 mV. The nanoparticles exhibited a sustainable drug release when studied for 60 minutes. The nanoparticles mentioned above were later formulated into a nanogel with the help of Carbopol 934 for transdermal application and subjected to *ex-vivo* permeation studies for 12 hours on excised rat's skin. The optimized formulation subjected to studies in rats showed a considerable enhancement in bioavailability (3 folds) compared with the NBH oral suspension.

Keywords: Nebivolol hydrochloride, Nanoparticles, Carbopol 934, Nanogel, Bioavailability

[a]. Department of Pharmaceutics, GITAM School of Pharmacy, Gandhi Institute of Technology and Management - GITAM, Rushikonda, Visakhapatnam-530045, Andhra Pradesh, India.
[b]. Faculty of Pharmacy, Gurunanak institutions technical campus, School of Pharmacy, Hyderabad-501506, Telangana, India.
[c]. Department of Pharmaceutics, GITAM School of Pharmacy, Gandhi Institute of Technology and Management - GITAM, Rushikonda, Visakhapatnam-530045, Andhra Pradesh, India.

***Corresponding Author**

E-mail: suvendu.gip@gmail.com

DOI: 10.31838/ecb/2022.11.10.010

INTRODUCTION

Several novel drug delivery systems have been the latest area of research due to their several benefits over traditional drug delivery methods. Transdermal drug delivery systems (TDDS) are known to be drug delivery systems designed to distribute medications via the skin at a set pace while avoiding the liver's first-pass effect [1]. Overcoming the epidermal barrier is the most challenging part of the transdermal medication delivery system; it proves itself as one of the ideal methods of drug delivery. There is proof that the skin's outermost layer, commonly known as the stratum corneum, was the rate-limiting phase in transdermal transfer [2]. Numerous strategies have methods to improve drug penetration via the skin's barriers to acquiring transdermal drug delivery [3].

Nanoparticles have excellent potential as cutting-edge medication carriers for transdermal drug delivery [4]. Due to their reduced size, Nanoparticles may ensure tight contact along the area of the stratum corneum, thereby maximizing the concentration of the medication encapsulated in it that enters the skin [5]. Adopting such colloidal carriers includes preventing the breakdown of unstable medications and controlling the rate at which pharmaceuticals are released [6]. Polymeric nanoparticles, which are solid particles with sizes between 1 and 1000 nm, have drawn much attention because of their durability and ease of surface modification [7].

Chitin, made up of N-acetyl glucosamine, can be alkaline-deacetylated to produce chitosan [8]. Chitosan to control drug release, despite being employed in medication delivery. So, to create drug release in a controlled manner involving chitosan-based formulations, researchers explored several chemical modifications of chitosan [9].

PLGA is a copolymer employed among numerous therapeutic devices that have received FDA approval [10]. By ring-opening co-polymerizing glycolic acid and lactic acid cyclic dimers, also known as 1,4-dioxane-2,5-diones, two distinct monomers, PLGA, are created. Additional polymer qualities are added by synthesizing random or block copolymers [11]. In PLGA, subsequent monomeric units (of glycolic or lactic acid) are bonded together during polymerization by ester bonds, resulting in the production of a linear, aliphatic polyester [12].

The cross-linked properties in the structure of carbopol make it a prospective candidate for its use in topical applications [13]. Carbopol gels with nanoparticles loaded with a drug studied for transdermal administration in earlier research [14]. The current

study aimed to create a transdermal Carbopol gel with chitosan-PLGA nanoparticles loaded with NBH.

NBH is an anti-hypertensive drug (BCS Class II) with a half-life (10 h) and is responsible for the treatment of hypertension symptomatically [15]. According to research, extended medication may cause side effects, including stomach irritation, ulcers, abdominal pain, and flatulence [16]. NBH is increasingly administered topically due to the adverse effects associated with oral treatment [17]. Additionally, the transdermal method of administration reduces side effects, prevents first-pass metabolism, improves patient compliance, and prolongs the duration of the plasma drug level. The current study used the nanoprecipitation/solvent displacement method to prepare chitosan-PLGA nanoparticles loaded with NBH. These nanoparticles were incorporated into Carbopol - 934 gel, and the newly formulated gel was tested both *in-vitro* and *ex-vivo* for transdermal delivery of NBH.

MATERIALS AND METHODS

Materials

MSN Labs in Hyderabad, India, gift sample provided NBH (purity > 99 percent). S.D. Fine Chemicals Ltd, India**,** provided Chitosan and PLGA**.** Other materials acquired were dialysis membranes from Hi-Media Labs Pvt. Ltd. in Mumbai and Carbopol 934 (C.P.) from RFCL Ltd, Mumbai, India**;** the remainder of the Chemicals and solvents were of analytical grade. They were, moreover, utilized without further processing or purification.

Preparation of NBH loaded chitosan-PLGA nanoparticles

Preparation of nanoparticles by nanoprecipitation / solvent displacement and freeze-drying method. Weighed all ingredients drug, PLGA and chitosan; the first drug dissolved in water; chitosan dissolved in 1% glacial acetic acid, PLGA in dichloromethane [18].

Then, the PLGA solution was added to the drug solution to the chitosan, mixed well, and sonicated the PLGA solution by adding the chitosan-drug solution to the probe sonicator for 15 seconds. Then the solution was kept for stirring for 30 minutes to evaporate dichloromethane. Finally, the solution was filled in centrifuge tubes of 50ml and centrifuged for 20 minutes at 8000 rpm. Taking the samples from the centrifuge and collecting supernatant detected the absorbance for entrapment efficiency [19]. The pellet was collected and freeze-dried for 12 hrs., and Nanoparticles were collected. Nanoparticles mentioned in **Table 1.**

Standardization of NBH loaded chitosan-PLGA nanoparticles

Drug entrapment efficiency estimation

100 mg of accurately weighed lyophilized nanoparticles with NBH were used for the study. They were taken from each formulation batch separately and stored in phosphate buffer (50ml). The pH of the solution was maintained at 6.8 for 24 hours with continuous stirring and centrifuged for 10 minutes at 3000 rpm. The supernatant was collected as filtrate, and the drug content in the obtained filtrate was determined using a UV-VIS spectrophotometer by recording the absorbance at 282 nm. The drug entrapment efficiency of nanoparticles was calculated by:[20]

$$\textbf{Drug entrapment efficiency}(\%) = \frac{\boldsymbol{Practical\ drug\ concentration}}{\boldsymbol{Theoritical\ drug\ concentration}} \boldsymbol{X100}$$

Determination of particle size and zeta potential

Before size analysis, the nanoparticles were sonicated in 10ml of pH 6.8 phosphate buffer for ten minutes to disperse them. Utilizing a particle size analyzer (Horiba SZ-100, Malvern Instruments, U.K), the produced homogenous nanoparticle was tested for their particle size and zeta potential.

Scanning electron microscopy (SEM)

SEM was used to study the morphology and shape of the particle surface. The method involves the application of concentrated suspension of nanoparticles with water on a slab and drying under a vacuum. The lyophilized nanoparticles were covered in a 20nm thick layer of gold and shadowed in a cathodic evaporate to determine surface morphology. Pictures were taken using the scanning electron microscope (Hitachi, S-3700N, Tokyo, Japan) operated at 20 kV.

Fourier transform-infrared (FTIR) spectroscopy

FTIR analysis was used to obtain the FTIR spectrum of the drug, polymer, and physical combination of the drug and polymers. About 5mg of the NBH chitosan nanoparticles were combined with 100mg of KBr IR powder before being compressed for three minutes under vacuum at a pressure of about 12 psi. The resulting disc was placed in an appropriate holder on an FTIR spectrophotometer (Shimadzu 8400S, Tokyo, Japan). The spectrum was examined over a range of 4000 - 400 cm-1 wave number in a scan for 12 minutes. The drug's identity was verified, and the drug's interaction with the carriers was discovered [21].

Differential scanning calorimetry (DSC)

Using a DSC (Shimadzu DSC 60, Tokyo, Japan), thermal analysis and the characteristics of the powder samples (NBH-optimized nanoparticles) were studied. An open aluminum pan contains 10mg of a sample heated under nitrogen between 0°C and 400°C with a scanning speed of 10°C/min for the analysis using Manges as a standard reference making it feasible to recognize physical changes in the preparation.

Powder X-ray diffraction (P-XRD)

Powder X-Ray diffraction analysis was used to assess the drug's crystalline state in the polymer sample and the captured X-ray spectra using Ni-filtered Cu Ka radiation. The diffractometer operated with a scintillation counter at 45 kV voltage and 40 mA current. Over a range of 5° - 40°C, the instrument was run at a continuous scanning speed of 4°/min. The samples were put into an aluminum sample holder, ground with a Wedgwood mortar and pestle, and packed evenly with a glass slide. The study made use of the tiniest size nanoparticle.

In-vitro drug release study

The technique of dialysis bag diffusion determined the in-vitro release of NBH from these produced nanoparticles. The dialysis bag at one end was filled with precisely weighed amounts of nanoparticles equivalent to 50 mg NBH and 5 ml of phosphate buffer, pH 6.8. The USP type II dissolution device included phosphate buffer maintained at a pH of 6.8, and the opposite side of the dialysis bag was knotted and submerged in it. The system is at a temperature of 37.5^{O}C and a speed of 100 rpm. The dissolving apparatus vessel serves as the receptor compartment, while the bag used up for dialysis serves as the donor compartment. Keep the sink condition throughout the experiment, 5ml aliquots were taken at regular intervals, and the same volume of fresh dissolving medium was added to the

dissolution vessel. The obtained aliquots were filtered and diluted appropriately to measure absorbance at 282 nm with a UV-VIS spectrophotometer [22].

Evaluation of in-vitro drug release kinetics

Utilizing a variety of significant mathematical models, including the zero-order, first-order, Higuchi, and Korsmeyer-Peppas models, the in-vitro drug release data were assessed kinetically [23].

Zero-order model: The zero-order model was studied using the equation $\mathbf{Qt = K_0t + Q_0}$, where; Qt represents the cumulative amount of drug release at a time "t" in hours, and Q0 is the initial amount of drug; K0 is the zero-order release constant.

First-order model: $\mathbf{Q_t = Q_0e^{Kt}}$ was the equation to determine the drug release, where Q_t represents the drug remaining released at time "t" in hours, and Q0 is the initial amount of drug; K is the first-order release constant.

Higuchi model: The equation to study the drug release per unit area was $\mathbf{Qt = KHt^{1/2}}$ used where Q_t corresponds to the amount of drug release per unit area at the time "t," and KH being the Higuchi constant.

Korsmeyer–Peppas model: The equation employed to study the fraction of drug release was $\mathbf{Q = KMt^n}$, where Q represents the fraction of drug released at a time "t" $\mathbf{K_M}$ represents kinetic constant, and n denotes release, indicative of the mechanism of drug release.

Preparation of nanogel of NBH loaded chitosan PLGA nanoparticles

In order to prepare the carbopol 934 solution, 100mg of carbopol 934 was dissolved in 6.5ml of deionized water and stirred continuously for 1 hour at 500 rpm using a magnetic stirrer (Remi Motors, India). The Carbopol mentioned above 934 solutions were then thoroughly blended with correctly weighed nanoparticles loaded with 50 mg of NBH. Finally, triethanolamine was added in weighed amounts to raise the pH of the mixture, including Carbopol 934, to produce the gel.

Characterization of Carbopol 934 gel containing NBH loaded chitosan-PLGA nanoparticles

Determination of pH

By inserting the glass electrode into the gel system of a digital pH meter (Slope, Model-15L-R), the manufactured gel's pH was measured and compared to a commercial formulation.

Viscosity measurement

A Brookfield DV III ultra V6.0 RV cone and plate viscometer was used to measure the gel's viscosity at a temperature of 25 ± 0.3^{O}C. Rheocalc V 2.6 was used to perform the calculations.

Ex-vivo permeation study

Skin preparation for ex-vivo permeation study

The *ex-vivo* permeation study for NBH from Carbopol 934 gel with NBH-loaded chitosan-PLGA nanoparticles was measured with the help of the skin of excised rats (210–300 g) (GNIP/CPCSEA/IAEC/2019/07). An animal hair clipper removes the hair from the animal's abdomen skin. A surgical scalpel is used to remove the fat stuck to the dermis side and remove the entire thickness of the skin. The skin was then wrapped in aluminum foil and refrigerated at 20^{O}C after being cleaned with a phosphate buffer with a pH of 6.8 and was used within 24 hours. [24]

In-vivo pharmacokinetic studies in rats:

Three groups of rats. Each Group with six rats for the study. Group II was treated with an oral suspension; Group III received an improved nanogel formulation, and Group I received a dose of the medication in its purest form. The rats were given sufficient contact with water and made to fast for 12 hours before the experiment. The subsequent day, sodium HPMC was used as a suspending agent to make NBH nanoparticles and oral suspensions, and pure medicines were administered orally to the two groups of rats. Each formulation had 100 milligrams of the medication. After administration, blood samples were taken by the orbit vein at intervals of 0.25, 0.50, 0.75, 1, 2, 3, 4, 6, 8, 10, 12, and 24 hours. Before the analysis, the blood samples were kept at -20°C in heparinized tubes and later promptly separated by centrifugation for ten minutes at 3000 rpm. The ezetimibe was later tested using the HPLC technique after extracting the plasma samples (Shimadzu Nexera SR, Tokyo, Japan). The deproteinization procedure was used in the processing of plasma samples. Each 200 mL sample of rat plasma received 400 mL of methanol. The mixtures were subjected to vortex for a short duration of 5 minutes (MS3, IKA, Germany) and then centrifuged for 5 minutes (Ultracentrifuge, Remi, India) at 3000 rpm. The supernatant was collected carefully and fed into an HPLC apparatus for further analysis in a volume of 20 L. Chemical stability studies cover the HPLC process in detail. Two batches of the plasma concentration-time profile were calculated, with the average and standard deviation at each point. A plot between concentration and time was created. Graphs were created by plotting plasma concentrations on the Y-axis and time on the X-axis to represent plasma concentrations. Software-generated AUC (0-t) and all other potential pharmacokinetic parameters for each formulation, including C_{max}, T_{max}, and half-life [25],[26].

***Ex-vivo* permeation study**

An abdominal rat skin was removed for the *ex-vivo* skin permeation investigation in a locally made Franz's diffusion cell with a diffusional area of 2.26 cm2. The stratum corneum was placed towards the donor compartment, while the dermis faced the receptor compartment. The donor compartment had the gel applied to the skin's surface, while the receptor compartment had phosphate buffer, 6.8 pH, inside it. The temperature of the diffusion cell was maintained, it continually swirled at 500 rpm, and aliquots were taken to observe under a UV spectrophotometer at 282 nm. After the experiment, the skin sample was removed from the Franz diffusion cell and cleaned with a phosphate buffer solution [27].

Permeation data analysis

Plotting the quantity of NBH that migrated from the gel throughout the eliminated skin over the course of time. The slope divided by the skin surface area was used to compute the permeation flux for gel using the following formula:

$\mathbf{K_P = J_{SS}/C_V}$

Where, K_P = permeability coefficient (cm/h), J_{SS} = flux (mg/cm /hr), A = area of the diffusion membrane (cm); C_V = initial concentration of the drug in donor compartment (mg)

Statistical analysis

The *in-vivo* data were analyzed for the differences in significance by employing paired samples t-test using Graph Pad Prism, Version 8.0.

RESULTS AND DISCUSSION

Preparation of NBH loaded chitosan PLGA nanoparticles

Nebivolol hydrochloride nanoparticles were prepared using different concentrations of chitosan, PLGA, and PLA by the Solvent displacement/ Nanoprecipitation method. A total of six

formulations were prepared, and all nanoparticle formulations appeared as fine white dispersion that showed no sedimentation. For the prepared Nebivolol hydrochloride nanoparticle, various evaluations test was performed.

Characterization of NBH loaded chitosan-PLGA nanoparticles

Drug entrapment efficiency

According to the findings, these nanoparticles' ability to trap drugs ranged from 85.36±0.89 to 94.31±1.51% (

Table 1) and NP-F6 was seen to have the highest drug entrapment efficiency (94.31±1.51%). The effectiveness of these formulations ability to entrap drugs was also measured, and it was noted that when chitosan content in the formulations decreased and PLGA content increased, the amount of drug entrapment increased. In the process of creating NBH loaded chitosan PLGA nanoparticles, the rising drug entrapment was also observed by gradual addition of PLGA.

Particle size and zeta potential

NBH loaded chitosan PLGA nanoparticles obtained had average particle diameter within 180-350nm **(**

Table 1). Particle size distribution of NBH loaded chitosan PLGA nanoparticles (NP-F6) formulated using 150mg chitosan and 100mg PLGA 1:5 % H_2O: dichloromethane is presented in (**Error! Reference source not found.**). With an increase in the amount of chitosan and a decrease in the amount of PLGA in their formulation, these nanoparticles' average particle diameter decreased. However, the addition and concentration of 1:5% H_2O: dichloromethane utilized in their manufacture also led to a decrease in the average particle diameter of the nanoparticles. This phenomena of smaller particles with the addition of PLGA may be caused by the polymeric gel shrinking as a result of increased cross-linking caused by the high cross-linker concentration (i.e., Chitosan, PLGA)

Table 1, the zeta potentials of various NBH loaded chitosan-PLGA nanoparticles fall between -52.7 and -30.4 mV. These findings made it very evident that adding more chitosan caused these nanoparticles' zeta potential to drop.

As seen in

Table 1: The composition chart for NBH loaded chitosan PLGA nanoparticles, their zeta potentials, average particle diameters, and drug entrapment efficiencies.

Formulations	Chitosan (mg)	PLGA (mg)	Antisolvent (5 ml Water): Solvent (10 ml dichloromethane)	Drug entrapment efficiency (%)	Average particle size (nm)	Zeta potential (mV)
NP-F1	50	300	1:2	85.36±0.89	350.40±1.63	-41.3±7.63
NP-F2	100	350	1:2	86.29±0.91	320.24±1.07	-52.7±7.91
NP-F3	150	400	1:2	87.25±1.36	297.51±0.76	-48.5±5.60
NP-F4	50	100	1:2	89.53±1.02	250.31±0.51	-47.8±4.16
NP-F5	100	100	1:2	91.67±1.07	247.92±0.54	-45.6±3.62
NP-F6	150	100	1:2	94.31±1.51	180.32±1.10	-30.4±7.68

SD± mean (n=3)

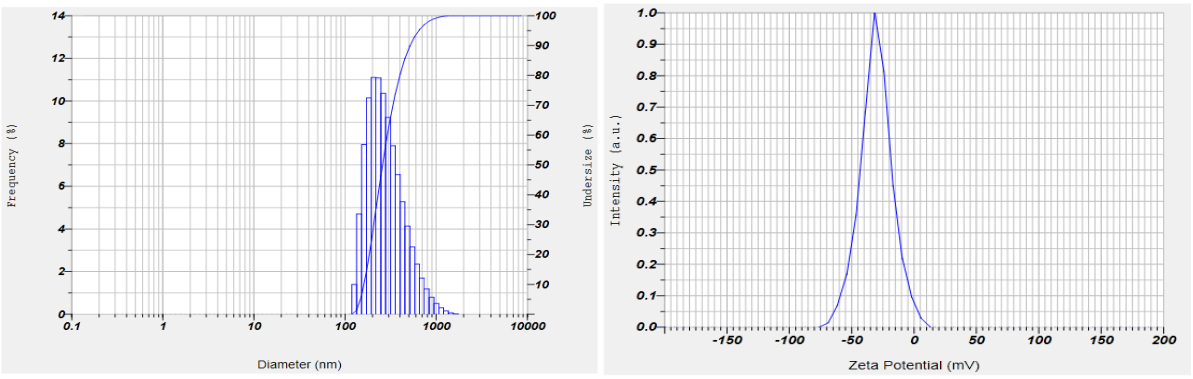

Figure 1. Particle size distribution, Zeta potential of NBH loaded chitosan PLGA nanoparticles (NP-F6)

SEM analysis

SEM analysis for the NBH loaded chitosan PLGA nanoparticles (NP-F6) was performed and photograph at 5000 X magnification **(**Error! Reference source not found.**)** showed that these particles appeared to be densely packed to each other. Particles were mostly in the nanoscale range and spherical in shape.

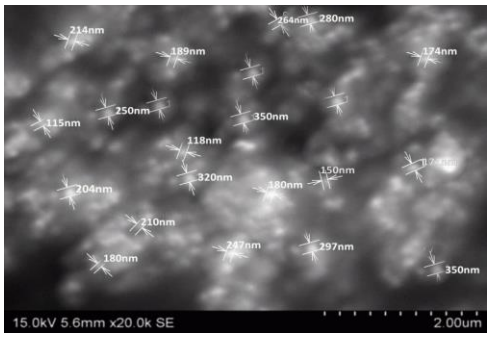

Figure 2. SEM image of Nebivolol hydrochloride - loaded chitosan-PLGA-nanoparticles (NP-F6)

FTIR spectroscopy

The FTIR spectrum of NBH is shown in (**Figure. 3)**, whereas the spectrum of NBH, chitosan, PLGA, and NBH-loaded chitosan PLGA nanoparticles (NP-F6) is shown in 3. The pure drug showed characteristic absorption bands at 3390.25 cm-1 (N-H Stretching), 1723.44 cm-1 (C=O stretching), 1516 cm-1 (C-N stretching), 2877(C-CH2 stretching) and the NP-F6 optimized formulation showed characteristic absorption band at 3339. 94 cm-1 (N-H Stretching), 1652 cm-1 (C=O stretching), 1458 cm-1 (C=N stretching), 3390 (C-CH2 stretching), and the compatibility of the NBH and polymer demonstrated by the FTIR spectra of pure NBH and the NP-F6 optimized formulation, which showed that all the NBH's distinctive peaks were present in the combination spectrum and there was no shift in peaks. Drugs and polymers did not interact physically or chemically and were found to be compatible since there is no incompatibility between them.

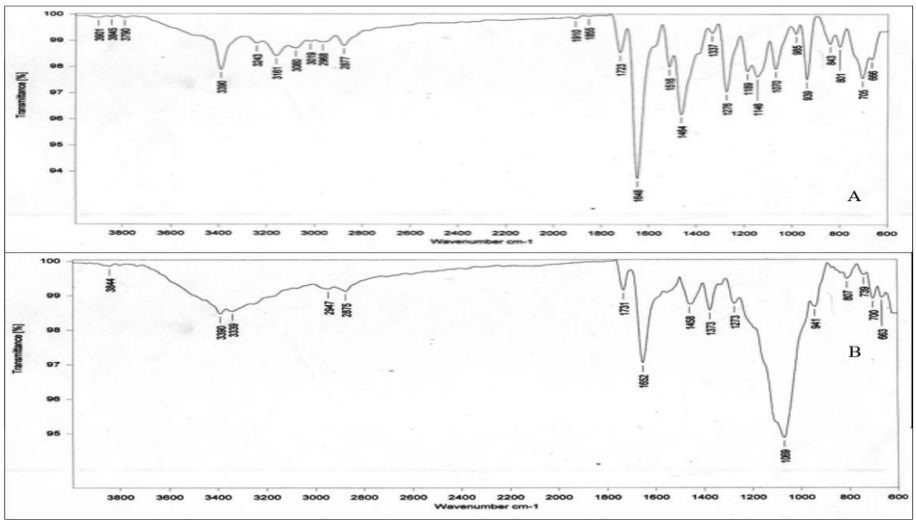

Figure 3. FTIR study of pure drug (A) and formulation NP-F6 (B)

DSC analysis

Figure. 4 shows thermograms of pure NBH and the NBH-loaded chitosan PLGA nanoparticles (NP-F6). The melting point of NBH is indicated by the thermal graph of pure NBH, which had distinct endothermic peaks at 229.31°C. Endotherms for NBH-loaded chitosan PLGA nanoparticles (NP-F6) at 225.21°C and 79.89°C. Thus, drugs and excipients used in the formulation of nanoparticles are compatible.

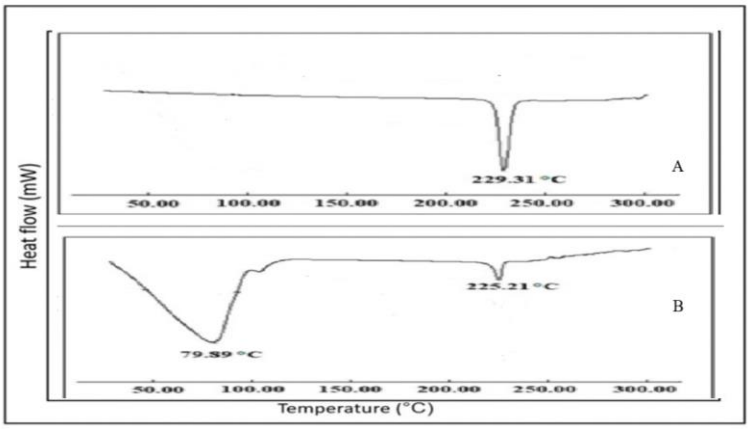

Figure 4. DSC thermograms of Nebivolol hydrochloride and NBH loaded chitosan PLGA nanoparticles (NP-F6)

P-XRD analysis

Figure. 5 illustrates the P-XRD patterns of NBH illustrates the P-XRD patterns of NBH-loaded chitosan PLGA nanoparticles (NP-F6). P-XRD of NBH revealed diffraction peaks with varying signal strengths at approximately 13.6°, 17.8°, 22.7°,

27.9°, 33.3°, and 41.2°, showing significant structural features of NBH. A slightly less pronounced peak was seen at 33.3° and 41.2° in the P-XRD pattern of NBH-loaded chitosan PLGA nanoparticles (F6), demonstrating that the drug (NBH) retains a small amount of its crystallinity in the nanoparticle formulation. The P-XRD pattern of NBH-loaded chitosan PLGA nanoparticles (F6) revealed a less pronounced peak at 33.3° and 41.2°, showing that the drug (NBH) retains a little percentage of its crystallinity in the nanoparticle formulation.

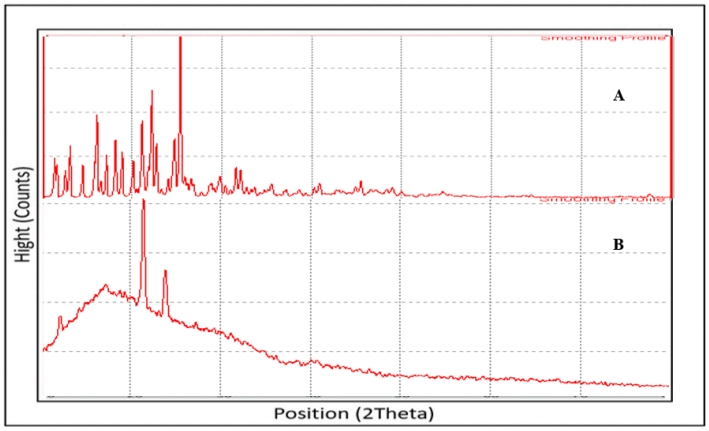

Figure. 5: PXRD analysis of the pure drug (A) and its formulation (NP-F6) (B)

In-vitro drug release

For the produced NBH-loaded chitosan PLGA nanoparticles, the *in-vitro* drug release was assessed using the dialysis bag diffusion technique in phosphate buffer, pH 6.8. Over 60 minutes, sustained drug release from the nanoparticles was observed (**Figure. 6**). All the formulated nanoparticle batches during the *in-vitro* study exhibited an initial drug release burst, which may have been caused by the presence of unbound or low banded capacity of pharmaceuticals on the surface of the prepared nanoparticles. The drug released from these NBH-loaded chitosan PLGA nanoparticles was computed and reported as cumulative percentage studies for 60 minutes and was found to be between 79.79+1.89 – 89.89+1%. The comparatively sustained release of NBH was evidenced in NP-F5 and NP-F6. However, NBH-loaded chitosan PLGA nanoparticles prepared using a higher concentration of PLGA indicated delayed drug release. Higher cross-linking is reported to be responsible for the delay in drug release [28].

The *in-vitro* drug release data of the prepared nanoparticles were evaluated kinetically using standard mathematical models. The correlation (R2) values were calculated to assess the accuracy for the best model fit, with values closer to 1 being the best model fit. The outcome of fitting the curve into several mathematical models was provided. All the prepared NBH chitosan PLGA nanoparticles obeyed the Korsmeyer-Peppas model throughout 8 hours when the individual R2 were compared. The range of release exponent (n) values for several NBH-loaded chitosan-PLGA nanoparticles used in *in-vitro* NBH release studies was 0.63 to 0.81, indicating an anomalous mechanism of diffusion for drug release. Both diffusions-controlled drug release is demonstrated by the anomalous diffusion mechanism of drug release [29].

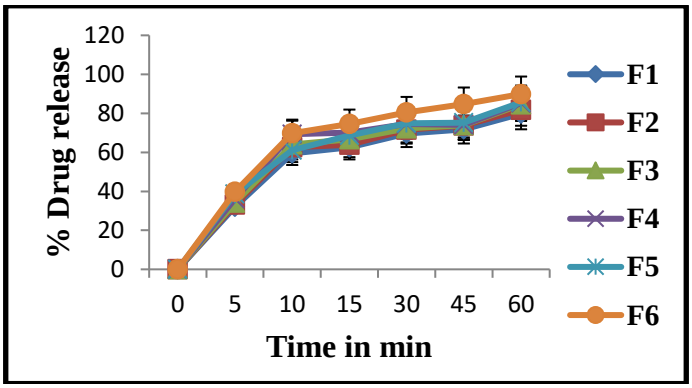

Figure. 6: The in vitro drug release from various Nebivolol hydrochloride -loaded chitosan-PLGA nanoparticles in phosphate buffer, pH 6.8 (mean ± S.D.; n = 3)

Table 2: In vitro Drug release of NBH loaded chitosan PLGA Particles

	NP-F1	NP-F2	NP-F3	NP-F4	NP-F5	NP-F6
Zero order	0.9779±0.013	0.9903±0.004	0.8483±0.004	0.8789±0.124	0.9002±0.011	0.9907±0.005
First order	0.8432±0.027	0.8573±0.027	0.9870±0.004	0.9657±0.013	0.9793±0.007	0.9864±0.002

Higuchi	0.9959±0.002	0.9896±0.005	0.9767±0.001	0.9830±0.002	0.9859±0.001	0.9584±0.002
Korsmeyer–Peppas	0.9883±0.010	0.9894±0.007	0.9873±0.002	0.9920±0.001	0.9908±0.0008	0.9924±0.001
Release exponent (n)	0.5679±0.006	0.7872±0.030	0.5855±0.003	0.6105±0.029	0.6039±0.038	0.6184±0.035

Preparation of Carbopol 934 Nanogel containing NBH loaded chitosan PLGA nanoparticles

A gel for transdermal application was made in the current study using NBH loaded chitosan PLGA nanoparticles and Carbopol 934, (NP-F6). We selected the formulation of nanoparticles to produce transdermal Carbopol 934 gel because it had a higher drug trapping capacity than the other nanoparticles made throughout the investigation.

Characterization of nanogel containing NBH loaded chitosan PLGA nanoparticles

pH

In the current study, a gel for transdermal application was made using NBH-loaded chitosan-PLGA nanoparticles and Carbopol 934, (NP-F6). We selected the formulation of nanoparticles to produce transdermal Carbopol 934 gel because it had a higher drug trapping capacity than the other nanoparticles made throughout the investigation.

Viscosity

Comparison between the viscosity of Carbopol 934 gel containing NBH loaded chitosan-PLGA nanoparticles was compared with plain NBH gel. Carbopol 934 gel with NBH loaded chitosan PLGA nanoparticles was found to have viscosity of 9840±1.632 cps, where as that of the plain gel (8529±2.054 cps) indicating the Carbopol 934 get of NBH nanoparticles to be more viscous.

Ex-vivo permeation study

Ex-vivo investigation on the skin penetration of produced Carbopol 934 gel with NBH loaded chitosan-PLGA nanoparticles and a plain NBH gel was conducted using excised mouse skin. Results from an *ex-vivo* skin permeation research showed that the drug penetration from both gels was sustained over a period of 12 hours(**Figure. 7**) [30]. The permeation in the case of Carbopol 934 gel was found to be 91.12±0.01, whereas in the case of plain NBH gel it was found to be (73.25±0.163).

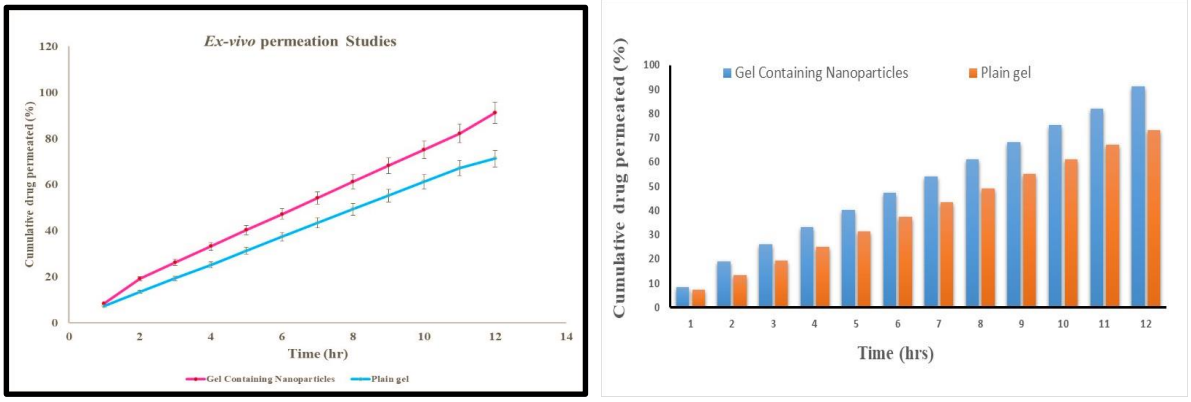

Figure. 7: The comparative ex-vivo drug permeation from Carbopol 940 gel containing NBH loaded chitosan PLGA nanoparticles and a plain NBH gel through excised mouse skin.

***In-vivo* animal studies**

Wistar rats were used in the in-vivo trials to show in-vivo bioavailability. The plasma concentrations of pure medication, suspensions, and nanogel were measured and compared after oral delivery. Comparing the nanogel plasma concentration profile to the suspension and pure medication in **table 3** showed a considerable improvement in drug absorption(**Figure. 8**) [31].

Table 3: Plasma drug concentrations of pure drug, oral suspension and NBH nanogel

Time (hrs)	0	0.25	0.50	0.75	1	2	3	4	6	8	10	12	24
Pure drug (µg/mL)	0	0.10	2.45	4.66	6.12	10.10	9.82	7.32	5.63	4.12	2.31	1.81	1.20
NBH Suspension (µg/mL)	0	3.01	6.01	8.32	15.11	21.69	18.32	13.21	9.37	6.33	4.03	2.13	0.85
NBH Nanogel (µg/mL)	0	16.99	22.26	32.32	51.01	65.10	48.12	33.33	22.12	17.45	11.23	3.89	0.96

There has been a notable improvement in the oral absorption of NBH as evidenced by the C_{max} and area under the curve (AUC) 0-24 hours values of nanogel, which were around three times greater than those of the oral solution. When NBH nanogel was delivered as a gel, the C_{max} was discovered to be 65.10 g/mL at 2 hours. The drug nanogel's adhesiveness, increased surface area as a result of smaller particle size, increased saturation solubility, which results in a higher concentration gradient between the blood and the lumen of the gastrointestinal tract, and increased dissolution velocity are all factors that contribute to the improvement in oral bioavailability. **Table 4** shows the different pharmacokinetic parameters.

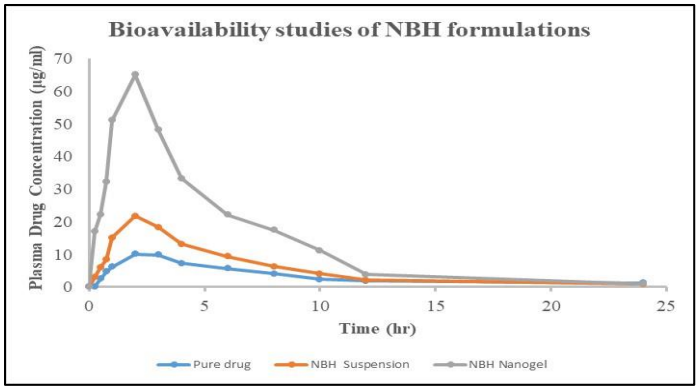

Figure. 8 Graph representing the bioavailability studies of pure drug, suspension and NHB nanogel

Table 4: Pharmacokinetic parameters of various NHB formulations

Parameter	Pure drug	Suspension	Nanogel
C_{max} (µg/mL)	10.12	23.14 µg/mL	69.54 µg/ml
t_{max} (hrs)	2.1	1.98 hrs	1.59 hrs
AUC (µg.hr/mL)	80.51	133.07	347.75
$t_{1/2}$	5.51 hrs	7.06 hrs	7.24 hrs
K	-0.126/hr	-0.098/hr	-0.095/hr

CONCLUSION

Based on the nanoprecipitation/solvent displacement approach, several NBH-loaded chitosan-PLGA nanoparticles were created. These nanoparticles had drug entrapment efficiencies that ranged from 85.37±0.93 to 94.31±1.51%. The formulation NP-F6, made with 150 mg of chitosan and 100 mg of PLGA, had the highest drug entrapment effectiveness (94.51%). NBH-loaded chitosan-PLGA nanoparticles reported having an average particle diameter and zeta potential of 180.32 nm and -30.40 mV, respectively. SEM, FTIR, DSC, and P-XRD tests were used to confirm the stability and physical state of the loaded NBH within the nanoparticles. The Carbopol 934 gel containing NBH-laden chitosan-PLGA nanoparticles was created for transdermal delivery of NBH. The in vitro drug release from all NBH-loaded nanoparticles revealed sustained drug release throughout one h, which followed the Zero order-Peppas model. pH and viscosity were two characteristics of the produced gel. *Ex vivo* skin permeation testing on abdominal rat skin revealed persistent NBH penetration through the carbopol 934 gel with NBH-loaded nanoparticles for 12 hours. NBH did, however, penetrate this Carbopol 934 gel formulation more quickly than it did the oral formulation. Therefore, it can be concluded that nano gel of NBH holds promise for delivering NBH transdermally with a simultaneous reduction in the frequency of application and improved compliance.

ACKNOWLEDGEMENT

The authors are thankful to the Management and principal of GITAM School of Pharmacy, GITAM (Deemed to be University) Visakhapatnam, for providing facilities to conduct research.

Funding: Nil

Authors contributions: All the authors have equally contributed to this manuscript.

Conflict of interests: The authors declare no conflict of interest.

REFERENCES

i. Mitchell MJ, Billingsley MM, Haley RM, Wechsler ME, Peppas NA, Langer R. Engineering precision nanoparticles for drug delivery. Nat Rev Drug Discov. 2021 Feb;20(2):101–24.

ii. Parhi R, Suresh P, Pattnaik S. Pluronic lecithin organogel (PLO) of diltiazem hydrochloride: effect of solvents/penetration enhancers on ex vivo permeation. Drug Deliv Transl Res. 2016 Jun;6(3):243–53.

iii. Hao J, Wang X, Bi Y, Teng Y, Wang J, Li F, et al. Fabrication of a composite system combining solid lipid nanoparticles and thermosensitive hydrogel for challenging ophthalmic drug delivery. Colloids Surf B Biointerfaces. 2014 Feb;114:111–20.

iv. Vitorino C, Almeida A, Sousa J, Lamarche I, Gobin P, Marchand S, et al. Passive and active strategies for transdermal delivery using co-encapsulating nanostructured lipid carriers: in vitro vs. in vivo studies. Eur J Pharm Biopharm Off J Arbeitsgemeinschaft fur Pharm Verfahrenstechnik eV. 2014 Feb;86(2):133–44.

v. Krishnaiah YSR, Al-Saidan SM, Chandrasekhar D V, Satyanarayana V. Bioavailability of nerodilol-based transdermal therapeutic system of nicorandil in human volunteers. J Control Release [Internet]. 2005;106(1):111–22. Available from: https://www.sciencedirect.com/science/article/pii/S0168365905001938

vi. Tiwari R, Pathak K. Nanostructured lipid carrier

versus solid lipid nanoparticles of simvastatin: comparative analysis of characteristics, pharmacokinetics and tissue uptake. Int J Pharm. 2011 Aug;415(1–2):232–43.

vii. Dumont VC, Mansur AAP, Carvalho SM, Medeiros Borsagli FGL, Pereira MM, Mansur HS. Chitosan and carboxymethyl-chitosan capping ligands: Effects on the nucleation and growth of hydroxyapatite nanoparticles for producing biocomposite membranes. Mater Sci Eng C Mater Biol Appl. 2016 Feb;59:265–77.

viii. Gupta A, Aggarwal G, Singla S, Arora R. Transfersomes: a novel vesicular carrier for enhanced transdermal delivery of sertraline: development, characterization, and performance evaluation. Sci Pharm. 2012;80(4):1061–80.

ix. Vitorino C, Almeida J, Gonçalves LM, Almeida AJ, Sousa JJ, Pais AACC. Co-encapsulating nanostructured lipid carriers for transdermal application: from experimental design to the molecular detail. J Control release Off J Control Release Soc. 2013 May;167(3):301–14.

x. Khan s, dubey n, khare b, jain h, jain pk. Preparation and characterization of alginate chitosan crosslinked nanoparticles bearing drug for the effective management of ulcerative colitis. Int J Curr Pharm Res [Internet]. 2022 Sep 15;14(5 SE-Original Article(s)):48–61. Available from: https://innovareacademics.in/journals/index.php/ijcpr/article/view/46372

xi. Lam PL, Gambari R. Advanced progress of microencapsulation technologies: in vivo and in vitro models for studying oral and transdermal drug deliveries. J Control release Off J Control Release Soc. 2014 Mar;178:25–45.

xii. Moore DJ, Rerek ME. Insights into the molecular organization of lipids in the skin barrier from infrared spectroscopy studies of stratum corneum lipid models. Acta Derm Venereol Suppl (Stockh). 2000;208:16–22.

xiii. Prausnitz MR, Langer R. Transdermal drug delivery. Nat Biotechnol. 2008 Nov;26(11):1261–8.

xiv. Draize JH, Woodard G, Calvery HO. Methods for the study of irritation and toxicity of substances applied topically to the skin and mucous membranes. J Pharmacol Exp Ther. 1944;82(3):377–90.

xv. Soliman MSM, Abdella A, Khidr YA, Hassan GOO, Al-Saman MA, Elsanhoty RM. Pharmacological Activities and Characterization of Phenolic and Flavonoid Compounds in Methanolic Extract of Euphorbia cuneata Vahl Aerial Parts. Molecules. 2021 Dec;26(23).

xvi. Shah j, patel s, bhairy s, hirlekar r. Formulation optimization, characterization and in vitro anti-cancer activity of curcumin loaded nanostructured lipid carriers. Int J Curr Pharm Res [Internet]. 2022 Jan 15;14(1 SE-Original Article(s)):31–43. Available from: https://innovareacademics.in/journals/index.php/ijcpr/article/view/44110

xvii. Fox LT, Gerber M, Plessis J Du, Hamman JH. Transdermal Drug Delivery Enhancement by Compounds of Natural Origin. Vol. 16, Molecules . 2011.

xviii. Barichello JM, Morishita M, Takayama K, Nagai T. Encapsulation of hydrophilic and lipophilic drugs in PLGA nanoparticles by the nanoprecipitation method. Drug Dev Ind Pharm. 1999 Apr;25(4):471–6.

xix. Sifaoui I, Díaz-Rodríguez P, Rodríguez-Expósito RL, Reyes-Batlle M, Lopez-Arencibia A, Salazar Villatoro L, et al. Pitavastatin loaded nanoparticles: a suitable ophthalmic treatment for Acanthamoeba Keratitis inducing cell death and autophagy in Acanthamoeba polyphaga. Eur J Pharm Biopharm Off J Arbeitsgemeinschaft fur Pharm Verfahrenstechnik eV. 2022 Sep;

xx. Hadizadeh F, Shamsara J. Qualitative Estimation of Drug Entrapment Efficiency in Polymeric Nano - Micelles Using Dissipative Particle Dynamics (DPD). Pharm Nanotechnol. 2017;5(2):154–61.

xxi. Song Y, Cong Y, Wang B, Zhang N. Applications of Fourier transform infrared spectroscopy to pharmaceutical preparations. Expert Opin Drug Deliv. 2020 Apr;17(4):551–71.

xxii. Can AS, Erdal MS, Güngör S, Özsoy Y. Optimization and characterization of chitosan films for transdermal delivery of ondansetron. Molecules. 2013 May;18(5):5455–71.

xxiii. Bhunia T, Giri A, Nasim T, Chattopadhyay D, Bandyopadhyay A. Uniquely different PVA-xanthan gum irradiated membranes as transdermal diltiazem delivery device. Carbohydr Polym [Internet]. 2013;95(1):252–61. Available from: http://europepmc.org/abstract/MED/23618267

xxiv. Wang C, Zhang J, Wang F, Wang Z. Extraction of crude polysaccharides from Gomphidius rutilus and their antioxidant activities in vitro. Carbohydr Polym. 2013 Apr;94(1):479–86.

xxv. Yaghini E, Tacconi E, Pilling A, Rahman P, Broughton J, Naasani I, et al. Population pharmacokinetic modelling of indium-based quantum dot nanoparticles: preclinical in vivo studies. Eur J Pharm Sci Off J Eur Fed Pharm Sci. 2021 Feb;157:105639.

xxvi. Gupta B, Rani M, Salunke R, Kumar R. In vitro and in vivo studies on degradation of quinalphos in rats. J Hazard Mater. 2012 Apr;213–214:285–91.

xxvii. Salimi A, Gobadian H, Sharif Makhmalzadeh B. Dermal pharmacokinetics of rivastigmine-loaded liposomes: an ex vivo-in vivo correlation study. J Liposome Res. 2021 Sep;31(3):246–54.

xxviii. Zaman M, Iqbal A, Haider Rizvi SF, Hussain MA, Jamshaid T, Jamshaid M. Chitosan based controlled release drug delivery of mycophenolate mofetil loaded in nanocarriers system: synthesis and in-vitro evaluation. Drug Dev Ind Pharm. 2021 Mar;47(3):477–83.

xxix. Sarkar T, Ahmed ab. Development and in-vitro characterisation of chitosan loaded paclitaxel nanoparticle. Asian J Pharm Clin Res [Internet]. 2016 Dec 1;9(9 SE-Original Article(s)):145–8. Available from: https://innovareacademics.in/journals/index.php/ajpc

r/article/view/12894

xxx. Silva-Abreu M, Espinoza LC, Halbaut L, Espina M, García ML, Calpena AC. Comparative Study of Ex Vivo Transmucosal Permeation of Pioglitazone Nanoparticles for the Treatment of Alzheimer's Disease. Polymers (Basel). 2018 Mar;10(3).

xxxi. Kasar pm, kale ks, phadtare dg. Nanoplex: a review of nanotechnology approach for solubility and dissolution rate enhancement. Int J Curr Pharm Res [Internet]. 2018 Jul 16;10(4 SE-Review Article(s)):6–10. Available from: https://innovareacademics.in/journals/index.php/ijcpr/article/view/28467